Scientific paper

Synthesis of MnO_2 on Activated Carbon and its Potential Application in the Adsorption of As(V) and Pb(II) in Aqueous Solutions

Roberto Contreras-Bustos,[1] E. Manríquez-Reza,[1] Jaime Jiménez-Becerril,[2,]* Melania Jiménez-Reyes[2] and Bibiana Cercado-Quezada[1]

[1] *Centro de Investigación y Desarrollo Tecnológico en Electroquímica S. C., Parque Tecnológico Querétaro, Sanfandila, Pedro Escobedo, C. P. 76703, Querétaro. México.*

[2] *Departamento de Química, Instituto Nacional de Investigaciones Nucleares, Apartado Postal 18-1027. C. P. 11801, Distrito Federal, México.*

** Corresponding author: E-mail: jaime.jimenez@inin.gob.mx*
Telephone: + (55) 53297200

Received: 08-02-2017

Abstract

The conditions for the synthesis of a material with MnO_2 (OMD) on activated carbon (AC) were studied. These conditions were: reaction time, temperature, stirring speed, concentrations of AC, H_2SO_4, and O_3 in solution, and particle size. Agglomerates on AC were observed by means of scanning electron microscopy (SEM) and microanalysis by energy dispersive spectroscopy (EDS) and revealed the presence of OMD deposited on the surface. The activation energy and the factor of frequency for the reaction were determined as $E_a = 1.2$ kcal/mol and $A = 2.2$. The value of E_a indicates that the precipitation of OMD on the AC was controlled by mass transfer in aqueous solution and the order of reaction was zero. The adsorption capacities of AC were $q = 14$ mg Pb(II)/g AC and $q = 9.1$ mg As(V)/g AC. Whereas, for the OMD/AC obtained in the following conditions: [AC] 1 or 2 g/L, particle size of AC of +0.59 mm, $[H_2SO_4]$ 1 or 2 mol/L, 25 °C, stirring speed 600 rpm, and $[O_3]$ 1.35 mol/L, the adsorption capacities were $q = 90.5$ mg Pb(II)/g OMD/AC and 25.4 mg As(V)/g OMD/AC. Therefore, the fixing of OMD on the surface of the AC greatly improved the removal of both Pb(II) and As(V) from aqueous solutions.

Keywords: MnO_2, Activated carbon, Lead, Arsenic, Adsorption

1. Introduction

Studies on absorbent materials for natural and anthropogenic contaminant ions, in both surface water and groundwater, remain of interest. Arsenic and lead ions have notable deleterious effects on human health. In Mexico, their presence has been detected in aquifers, especially in the north of the country.[1] They cause various diseases including skin diseases, bone diseases and diseases in other vital organs. Moreover, they can lead to death when high-dose exposure is continuous. Thus, it is important to find efficient alternatives for the removal of these ions from water and to reduce the risks to human health.

Arsenic is present in the atmosphere, soil, rocks, natural water and organisms. Most environmental problems related to arsenic contamination are due to mobilization under natural conditions. For human beings, arsenic has an important impact in the form of mining, burning fossil fuels and use of arsenic-containing pesticides, herbicides and livestock feed.[2] The presence of arsenic in water usually indicates nearby mines or metallurgical industries in operation or agricultural areas where materials with arsenic are used.[3] The average levels of arsenic in groundwater are between 0.001 and 0.002 mg/L; however, in areas with volcanic rocks and sulfide ore deposits, these levels are > 3 mg/L. The World Health Organization (WHO) established that the arsenic in water for human consumption should not exceed 0.01 mg/L.[4] This is a provisional value given the uncertainty of the risks associated with a lower concentration of arsenic; in 1984, the WHO had set limit value of 0.05 mg/L. The U.S. Environmental Protection Agency (EPA) indicates a maximum permissible limit concentration of arsenic of 0.01 mg/L for drinking water.[5] The Mexican official standard is a maximum permissible limit concentration of 0.025 mg/L.[6]

Lead is present in the environment, including in the air, dust, soil and water. This element and its compounds are widely used for batteries, pigments, ammunitions, weldings, pipes, coated cables and bearings. Other sources of contamination are mining and smelting waste, petrol and paintings.[7] The maximum permissible limit concentration of lead in drinking water established by the WHO for water is 0.01 mg/L. Per the U.S. EPA, the limit is 0.015 mg/L, though it is also 0.01 mg/L according to the Mexican official standard.[4–6]

There are several technologies for the treatment of contaminated water with arsenic and lead ions such as coagulation-filtration, chemical precipitation, ion exchange and lime softening, among others.[7–15] In recent years, research has been conducted on low-cost and easily obtainable materials that may be useful for absorbing heavy metals. Among these materials are: activated charcoal, zeolites, chitosan, clays, biocarbon, and sand.[16–19] To increase the adsorption capacity of these natural adsorbents materials, changes to their surfaces have been proposed. For lead removal, several possibilities have been tested, including: manganese dioxide onto zeolites, sand or resins, cellulose, carbon nanotubes, pretreated clinoptilolite, and graphene.[20–25] Regarding arsenic removal, the deposition of MnO_2 (OMD) onto polystyrene resins, zeolites and MCM-41 has been proposed.[10,11,26–30]

Oxidation of manganese ions by ozone in an aqueous solution has been widely studied, and it is a feasible alternative for the production of OMD.[31] Ozone is one of the strongest oxidants and offers the advantage of not introducing unwanted specimen into the system; therefore, its use guarantees the purity of the product obtained. OMD obtained *via* this method has better characteristics than if it was produced *via* other methods. Moreover, this type of OMD exhibits good behavior for ion exchange.[32–34] Preferentially, OMD exchanges with other ions in the order Pb(II) > Zn(II) > Cd(II) > Tl(I).[35]

Activated carbon (AC) is a low-cost adsorbent that, depending on the conditions of the adsorbate, can be used in a wide pH range. Its adsorption capacity stems not only from its surface area but also its physicochemical nature, i.e. properties obtained during the activation process.[36–38] Manganese dioxide obtained by specific conditions of ozonation (OMD) has better adsorption capabilities than if it was obtained by electrolytic or chemical methods. The size of the OMD obtained by direct precipitation is relatively small. An interesting option is the use of a supporting material such as AC to obtain a larger material useful in traditional adsorption columns. The synthesis of OMD consumes electricity for the formation of ozone; however, with the use of alternate energy sources (i.e., solar), costs could be mitigated. Manganese sulfate can be obtained during the acid leaching of manganese ore, whose oxidation with ozone can be directly applied in the presence of AC. The cost of obtaining OMD from manganese ore is comparable to that of obtaining it by the electrolytic method. In addition, OMD/AC provides the features for adsorption of Pb(II) or As(V); furthermore, the reversibility of adsorption has been proved for cadmium(II) and zinc(II) with an acid solution at pH 1–2.[35]

The present investigation proposes the synthesis of an adsorbent material, which consists of OMD supported by AC to examine whether its physical and chemical characteristics are suitable for the adsorption columns used in water purification. The specific aims of this research are: 1) to establish the best conditions for the synthesis of OMD/AC, 2) to characterize the material, and 3) to determine the adsorption capacity of the material for Pb(II) and As(V) ions.

2. Experimental

2. 1. Synthesis of MnO_2/AC

For the synthesis of the OMD, $MnSO_4$ (Karal S. A. de C. V., reagent grade) and H_2SO_4 (Baker, reagent grade) were used. Granular AC type CAGR 8 × 30 (Clarimex), certified by the National Science Foundation and previously characterized was used.[39] The AC is of lignite origin, is activated by vapor steam, has an average pore diameter of 3.5 nm and has a surface area of 664 m^2/g. The determinations using the inductively coupled plasma (ICP-OES) spectrometry (Perkin Elmer, Optima 3300 DV) gave the following data: Al: 256 mg/kg, Si: 143 mg/kg, Na: 1085 mg/kg, K: 300 mg/kg, Ca: 872 mg/kg, Sr: 756 mg/kg and V: 14 mg/kg.

OMD synthesis was performed *via* the oxidation by ozonation of Mn(II) in aqueous solution. A solution of 1 g/L of $MnSO_4$ and 1 mol/L H_2SO_4 was prepared with deionized water and was deposited in a glass reactor with 2 g of AC. The system was stirred to 600 rpm for 2 h, and the temperature was controlled at 25 °C. A gaseous mixture of O_2/O_3, produced in an ozone generator (PCI Ozone & Control Systems, mod. GL-1) supplied with oxygen was introduced into the reactor. Samples were taken at 0, 30, 60, 90 and 120 min of reaction. The samples were filtered and the solid was washed with 100 mL of deionized water. These samples were identified as OMD/AC. Finally, the samples were stored in a desiccator. Liquid samples were analyzed by ICP-OES.

The base conditions for the synthesis were: temperature, 25 °C; stirring, 600 rpm; concentration of AC, 2 g/L; [H_2SO_4], 1 mol/L; [O_3] in solution, 1.32 mol/L; and particle size of AC, +0.59 mm. Each parameter was independently varied in order to find out the best adsorption capacity of the material for Pb(II) and As(V) ions. The temperature ranged from 25 to 70 °C; the concentration of AC from 0.5 to 5 g/L; the ozone concentration in solution from 0.35 to 1.65 mol/L; the concentration of H_2SO_4 from 1 to 3 mol/L; the stirring speed from 200 to 800 rpm; and the particle size from AC of +0.59 to +1.6 mm.

The resulting solid material was characterized using scanning electron microscopy (SEM) and microanalysis by Energy Dispersive Spectroscopy (EDS) (Jeol, mod. JSM35CFLV) to corroborate the presence of manganese deposits on the surface of the AC and to identify other elements in the samples.

2. 2. Adsorption of Lead and Arsenic

The solutions used for the experiment were one of lead and one of arsenic, each with a concentration of 1 g of the element per liter. They were prepared with $Pb(NO_3)_2$ (Baker, reactive grade) and $Na_2HAsO_4 \cdot 7H_2O$ (Mallinckrodt Chemical Works, reagent grade) in deionized water. These solutions were stored in polyethylene containers. The stock solutions were diluted up to a concentration of 100 mg/L for the adsorption experiments. 0.1 g of OMD/AC prepared in specific conditions was put in contact with 100 mL of these solutions. For lead, the adsorption experiments were carried out at pH = 4.7 to avoid the precipitation of lead as hydroxide. According to the chemical species diagram at pH = 4.7 lead is present only as Pb(II).[40] Arsenic experiments were done at pH 8.8, when As(V) can be found as the anionic species 30% $(H_2AsO_4)^-$. Contact was done in an isothermal bath with stirring at 300 rpm at 25 °C for 24 h.

After the contact the solutions were filtered and a nitric acid solution added to maintain the pH < 2, the samples were stored in polyethylene bottles. Lead was then present as Pb(II) and As(V) was ca. 70% as H_3AsO_4 and ca. 30% $H_2AsO_2^{4-}$ all of which are water soluble.[40] These samples were analyzed for Pb(II) or As(V) using ICP-OES. The OMD/AC was flushed with 100 mL of deionized water, dried at temperatures up to 35 °C for 12 h and stored in a desiccator with silica gel.

To determine the influence of each individual condition on the synthesis of OMD/AC, the adsorption capacity of the material for Pb(II) and As(V) was tested using the material obtained under different stirring speed, ozone concentration, acidity, AC concentration, temperatures, and AC particle sizes.

The equation used for the calculation of the adsorption capacity was:

$$q = \frac{(c_i - c_f) * V}{m} \tag{1}$$

where q is the adsorption capacity (mg ion/g adsorbent), m is the mass of the adsorbent (g), C_i is the initial concentration of ions in solution (mg/L), C_f is the final concentration of ions in solution (mg/L) and V is the volume of the solution (L).[41] The adsorption capacity of AC for Pb(II) and As(V) was measured as well.

3. Results and Discussion

3. 1. OMD/AC Synthesis

3. 1. 1. Stirring Speed

The values of Mn(II) when remaining in solution for the same amount of time are very similar (Table 1); this means that the parameter does not significantly alter the oxidation rate reaction. It can be deduced that the mass-transfer phenomenon in that range of stirring speed is not important. A slight increase of Mn(II) deposition was observed, however, at a stirring speed of 800 rpm at 120 minutes of reaction. Mn(II) probably spreads in the AC by means of electrostatic attraction with the electrically charged sites of the surface, and then, when ions are already deposited, oxidation occurs to form OMD.

3. 1. 2. Ozone Concentration

Table 1 shows the influence of the concentration of ozone on the oxidation rate reaction of Mn(II) in the presence of AC. The oxidation rate increases in relation to the concentration of ozone in solution. The best conditions for attaining the lowest concentration of Mn(II) in solution are 1.35 mol/L and 120 min of reaction.

With $t > 90$ min of ozonation and a concentration of O_3 of 1.65 mol/L, a re-dissolution of manganese ions was

Table 1. Manganese concentration (mg/L, in italics) remaining in solution, with respect to stirring speed (rpm), ozone concentration (mol/L) and reaction time (min).

t	**Stirring (rpm)**				**[O_3] (mol/L)**			
(min)	**200**	**400**	**600**	**800**	**0.35**	**1.32**	**1.35**	**1.65**
0	1000	1000	1000	1000	1000	1000	1000	1000
30	920	826	834	816	890	834	790	680
60	770	705	711	642	780	670	590	360
90	608	550	508	410	670	508	388	38
120	423	380	377	184	565	340	180	299

observed due to the oxidation of the ions Mn(IV) up to Mn(VII), revealed by the characteristic violet color. In accordance with the Pourbaix diagram at the experimental pH, Mn(II) can be oxidized to MnO_2 and subsequently to MnO_4^-.[42] The calculation of the order of reaction was performed with the following equation:

$$\log(-r_A) = log\ k + nlog\ C_A \tag{2}$$

where r_A expresses the variation of the concentration of a species (Mn(II)) with respect to time, C_A is the concentration of ozone, k is the rate constant and n) is the order of reaction.

The graphics (not included) corresponding to 30, 60 and 90 min of stirring and ozone concentrations of 0.35 to 1.35 mol/L have slopes ≈ 0.5; this is considered a zero-order reaction. The value of $\log(-r_A)$ tended to be higher, indicating a change in slope, only in the case of 90 min and 1.35 mol/L ozone. For the lowest concentrations of ozone in solution the mass-transfer phenomena have more influence in the process than the chemical reaction itself during oxidation of Mn(II). However, as the concentration of dissociated ozone increases, the chemical reaction becomes more important.[43]

3. 1. 3. Sulfuric-acid Concentration

The oxidation rate reaction of Mn(II) decreases with the increase in sulfuric-acid concentration (Table 2). For the range of acidity used, the best condition was 1 mol/L H_2SO_4. Moreover, the start-up time for reaction increases when the acid concentration increases. The low rate of oxidation with high concentrations of H_2SO_4 may be due to a competition between protons and Mn(II) ions for the active sites of AC. Another explanation is that the low rate of oxidation is due to the high viscosity observed with a high concentration of acid.

3. 1. 4. AC Concentration

As can be seen in Table 2, the values corresponding to the change of Mn(II) for the oxidation reaction without AC have tendency very similar to that of the tests carried out with the presence of AC. Rodríguez-Santillan et al. mention that the AC favors the decomposition of O_3 in solution even at low pH;[44] however, in the conditions of the present work, this was not observed.

According to the calculations done in accordance with Equation 2, the oxidation reaction is of zero-order with respect to this variable. This means that, in the interval of the AC used, this parameter does not have a significant influence on the rate of oxidation of Mn(II) by ozone.

3. 1. 5. AC Particle Size

The rate reaction is quite similar for the three particle sizes, namely 0.59, 1.19 and 1.6 mm (Table 3). Thus, it can be deduced that this variable does not influence the process of oxidation of Mn(II).

3. 1. 6. Temperature

Increasing temperature to 70 °C and reaction times to greater than 60 min favors oxidation; for lower temperatures, there was no noticeable difference (Table

Table 2. Manganese concentration (mg/L, in italics) remaining in solution, with respect to initial sulfuric-acid concentration (mol/L), quantity of activated carbon (g) and reaction time (min).

t	**[H_2SO_4] (mol/L)**			**AC (g)**					
(min)	**1**	**2**	**3**	**0**	**0.5**	**1**	**2**	**3**	**5**
0	1000	1000	1000	1000	1000	1000	1000	1000	1000
30	834	959	992	743	723	761	834	787	742
60	711	852	925	592	549	629	711	651	657
90	508	654	848	439	351	392	508	489	448
120	377	452	805	255	143	269	377	246	276

Table 3. Manganese concentration (mg/L, in italics) remaining in solution, with respect to the particle size of activated carbon (mm), temperature (°C) and reaction time (min).

t	**Particle size (mm)**			**Temperature (°C)**			
(min)	**0.59**	**1.19**	**1.6**	**25**	**40**	**60**	**70**
0	1000	1000	1000	1000	1000	1000	1000
30	834	751	793	834	840	876	876
60	711	589	618	711	666	643	647
90	508	404	412	508	469	419	417
120	377	242	251	377	251	221	60

3). Similar observations have been reported previously.[35]

The *k* values for temperatures of 25, 40, 60, and 70 °C were calculated considering the slopes of the graphs of Figure 1A. These values were used to determine the activation energy by the Arrhenius linear equation:

$$\ln k = \ln A - E_a / RT \tag{3}$$

where *k* is the rate constant, *A* is the factor of frequency, E_a is the activation energy (kcal/mol), *R* is the universal constant of the gases, and *T* is temperature (K).

Figure 1B shows a graph in which the activation energy and the factor of frequency are the slope and the intercept of the line, respectively. These values are E_a = 1.2 kcal/mol and *A* = 2.2. According to Peters and Bolton, E_a values under 4.7 kcal/mol and occasionally under 2.3 kcal/mol correspond to mechanisms controlled by mass-transfer in an aqueous solution;[45] therefore, deposition of MnO_2 on AC can be considered as such. Thus, temperature does not influence the process of MnO_2 precipitation.

3. 2. Characterization by SEM

Figure 2 shows typical images obtained by SEM. In the micrograph taken to the scale of 150× and 100 µm (a), fine particles were observed on the AC. Yet, in the micrograph taken to the scale of 2000× and 10 µm (b), agglomerates of OMD were deposited on the surface of the AC. The EDS (c) revealed the presence of manganese and silicon, which were located on the AC surface.

When low ozone concentrations were used for synthesis, the images showed less deposits of manganese on the AC than on samples synthesized with high concentrations of ozone; thus, the increase of ozone can be said to favors precipitation.

3. 3. Adsorption of Pb(II) in OMD/AC

Table 4 shows the influence of different conditions on the synthesis of OMD/AC in terms of the composite's adsorption capacity for lead. This adsorption capacity increases with the stirring speed, probably due stirring speed's creation of more homogeneous deposits of OMD. However, the OMD/AC formed at 800 rpm does not present the best features for removing Pb(II), because the dissemination processes do not favor the solid-liquid interface or because the contact time between the particles of OMD and AC was reduced. Moreover, this condition of synthesis could also create fractures of AC particles; hence, the OMD deposited on them may become detached.

The adsorption capacity of lead in the OMD/AC increased when the concentration of ozone used in the synthesis of the material was changed from 0.35 to 1.32 mol/L (Table 4); however, with higher concentrations, this adsorption capacity decreased. This can be explained by a partial re-dissolution of manganese as MnO_4^- during synthesis, and resulting decrease of manganese as an oxide on the surface of the AC, which is the chemical species that allows for efficient adsorption.

Table 4 also shows the influence of sulfuric-acid concentration. When the concentration of the acid reaches 2 M, the formation of γ-MnO_2 is promoted, thereby increasing adsorption capacity. A higher concentration of sulfuric acid (3 mol/L) favors the formation of Mn(III), an intermediate species between Mn(II) and MnO_2.[35] In addition, in this case, the decrease of manganese as an oxide on the surface of the AC reduces the lead adsorption capacity of the material.

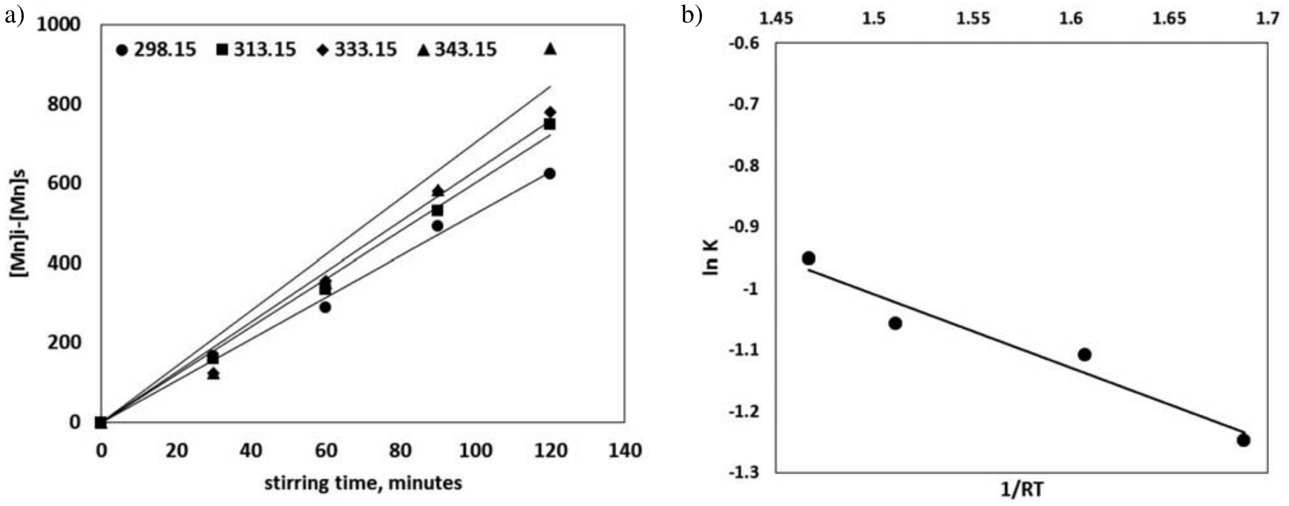

Figure 1. a: Initial manganese *(mg/L)* minus manganese remaining in solution as a function of stirring time. The slopes are: 5.24, 6.02, 6.33, and 7.04 for 298.15, 313.15, 333.15, and 343.15 K, respectively. b: Estimation of activation energy by means of the Arrhenius equation. Ln K = –1.2*(1/RT) + 0.797 (R2 = 0.94)

The adsorption capacity of Pb(II) by OMD/AC decreases when the concentration of AC used in the synthesis of the material increases (Table 4), for the amount of OMD present in the adsorbent material is proportionally smaller.

The best adsorption capacity with respect to the temperature of the formation of the OMD/AC was 82.7 mg Pb(II)/g in the material prepared at 40 °C. The adsorption capacity of the material is reduced at higher temperatures during synthesis. Umetsu et al. reported a similar behavior; they observed that OMD does not present adsorption for a synthesis at 70 °C.[46] Although there are significant deposits of OMD in the synthesized material at that temperature, the results indicate that the main factor responsible for the removal of Pb(II) is AC.

Regarding particle size, the best adsorption capacity (85.8 mg Pb(II)/g OMD/AC) was obtained using the synthesized material with the largest AC particle, because it presents more deposits of OMD on the surface. In the intermediate-sized synthesized material with AC, the removal of Pb(II) was reduced because of small amount OMD deposits, which was observed in the micrographs for particles sizes of 0.59 and 1.6 mm. Finally, when using the smallest AC particles, the Pb(II) removal was also high (71.7 mg Pb(II)/g OMD/AC); the presence of few OMD deposits, the adsorption capacity increased if the size of the AC was reduced.

The conditions of synthesis of OMD/AC with the maximum adsorption capacity of Pb(II) are: 2 mol/L of sulfuric acid, temperature at 25 °C, stirring at 600 rpm, AC par-

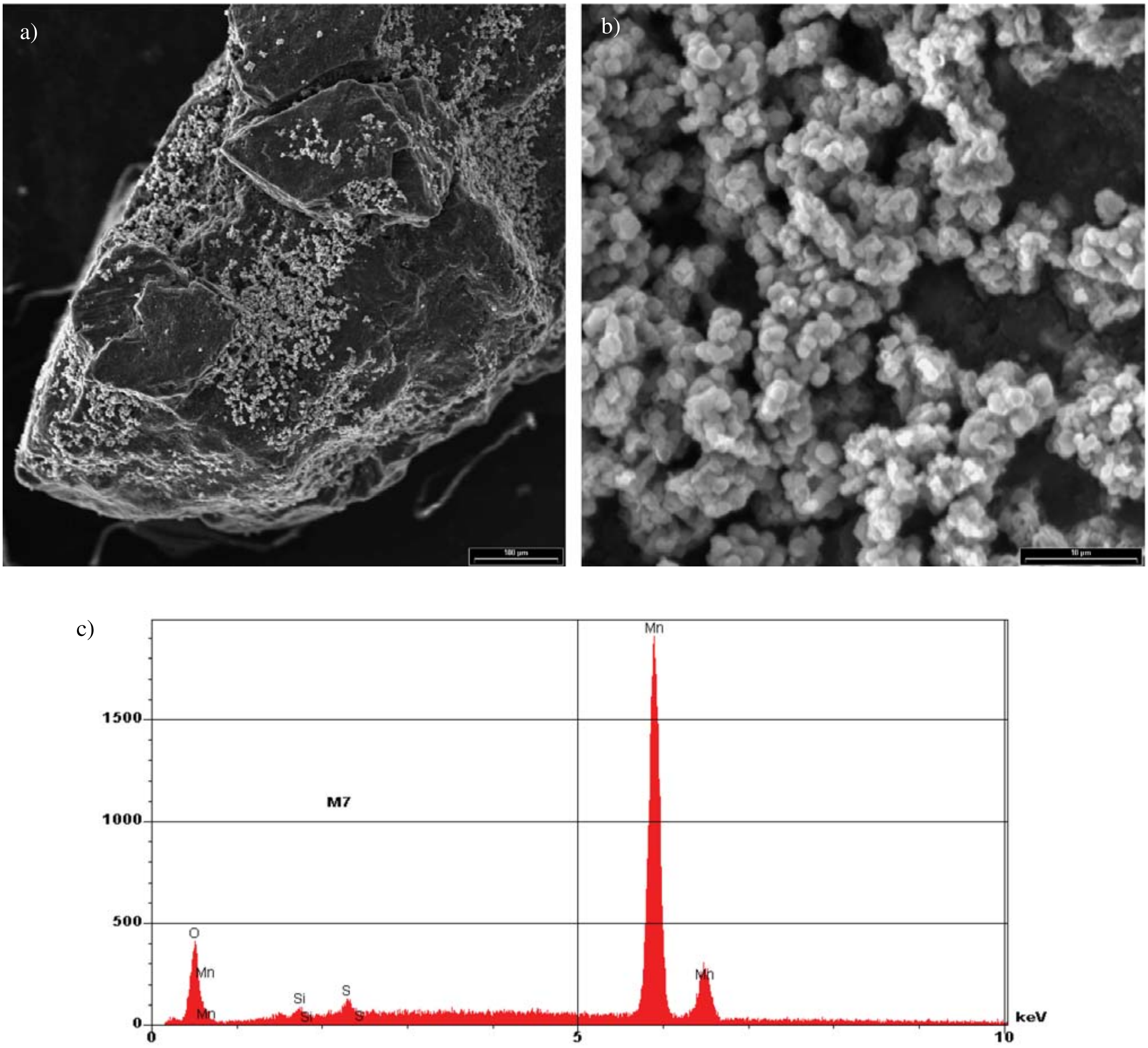

Figure 2. Typical micrographies of the synthetized materials. (a) 150×, (b) 2000×, (c) EDS obtained in micrography.

Table 4. Adsorption capacities of OMD/AC for Pb(II) and As(V) with respect to different synthesis parameters for OMD/AC. Initial concentrations = 100 mg/L. Without OMD, q_0 = 14.0 mg Pb(II)/g AC and q_0 = 9.1 mg As(V)/g AC.

Synthesis parameters for OMD/AC	Condition	*q* (mg Pb(II)/g OMD/AC)	*q*(mg As(V)/g OMD/AC)
Temperature (°C)	25	71.7	4.3
	40	82.7	19.0
	60	70.7	18.8
	70	71.0	8.0
Stirring (rpm)	200	54.6	17.3
	400	60.9	18.5
	600	71.7	4.3
	800	39.3	4.7
[O_3] (mol/L)	0.35	40.0	5.6
	1.32	71.7	4.3
	1.35	56.6	1.0
	1.65	76.8	4.5
[AC] (g/L)	0.5	84.6	17.6
	1.0	81.4	25.1
	2.0	72.0	4.3
	3.0	20.3	1.8
	5.0	44.0	7.3
[H_2SO_4] (mol/L)	1.0	71.7	4.3
	2.0	90.6	16.5
	3.0	34.7	19.5
Particle size of AC (mm)	0.59	71.7	4.3
	1.19	49.5	19.7
	1.60	85.8	10.1

ticle size at +0.59 mm, [O_3] 1.35 mol/L, and [AC] 2 g/L. The adsorption-capacity value in these conditions is 90.5 mg Pb(II)/g OMD/AC; for AC, however, it is 14 mg Pb(II)/g AC. Therefore, the fixing of MnO_2 on the surface of the AC greatly improves the removal of ions Pb(II) of aqueous solutions.

3. 4. Adsorption of As(V) in OMD/AC

The results of the experiments carried out to determine the adsorption capacity of As(V) on the material in each of the conditions of synthesis was calculated in the same way as described for lead, following Equation 1 and determining the influence of each individual parameter. The values obtained are shown in Table 4.

At the experimental pH (8.8), As(V) can be found as an anionic species $H_2AsO_4^{2-}$.[40] Even if the OMD is considered a cation exchanger, the use of this material to remove As(V) has been reported in the literature.[47–49]

Table 4 shows that the adsorption capacity was better with a slow stirring speed during synthesis (200 and 400 rpm); the highest value obtained was for 400 rpm (18.5 mg As(V)/g OMD/AC). The increased stirring speed resulted in a drastic decrease in the adsorption capacity because of fewer deposits of manganese oxide, which is responsible for adsorption.

The ozone concentration used for the synthesis of OMD/AC does not have a significant influence on the adsorption capacity for arsenic ions. The maximum adsorption capacity is less than 6 mg As(V)/g OMD/AC for a concentration of O_3 = 1.65 mol/L. This behavior is different from that observed with the adsorption of Pb(II) for the same parameter because the mechanism of ion exchange of the OMD is different for cations and anions.

The adsorption capacity of As(V) in OMD/AC depends on H_2SO_4 concentration; it increased when that concentration increased from 1 to 3 M. The best adsorption capacity was 19.5 mg As(V)/g OMD/AC for 3 mol/L of H_2SO_4. The increase of the anion exchange of the OMD is given by the presence of sulfate ions on the surface, which allowed for a greater exchange of anions. However, the variation of the adsorption capacity between 2 and 3 mol/L did not produce noticeable changes. The amount of OMD deposited on the AC decreased when the concentration of the acid increased; therefore, the adsorption of As(V) also decreased.

An adsorption capacity of 25.1 mg As(V)/g OMD/AC was obtained when the concentration of AC was 1 g/L; with higher concentrations, smaller values were obtained. This behavior is similar to that observed for Pb(II), and similarly related to the amount of OMD present in the adsorbent material, which is proportionally smaller.

With respect to the temperature of the synthesis of OMD/AC, the tendency is the same for the As(V) as for the Pb(II). At low synthesis temperatures the adsorption capacity was higher showing the best results at 40 °C, although it remained virtually constant up to 60 °C, with 19.0 and 18.5 mg As(V)/g OMD/AC, respectively. At 70 °C a significant decrease in the adsorption capacity was observed. The reduction of the ion-exchange capacity of OMD/AC meant that the capacity for retention of the material decreased when more deposits of manganese were present in the adsorbent material.

The adsorption of As(V) with respect to particle size displayed the opposite behavior as the adsorption of Pb(II). In this case, with the smallest particle size, the adsorption capacity was the lowest. The sample used for this experiment probably had few OMD deposits, so the main adsorbent was AC. For other particle size, OMD deposits were confirmed; however, no high adsorption capacity was observed. The highest adsorption capacity was 19.7 mg As(V)/g, for a particle size of AC = +1.19 mm. The removal of As(V) does not present a clear tendency with regard to the particle size used for the synthesis of OMD/AC in the present work.

The best adsorption capacity obtained was 25.4 mg As(V)/g OMD/AC with a material prepared as follows: AC concentration 1 g/L, temperature at 25 °C, stirring speed at 600 rpm, AC particle size at +0.59 mm, [O_3] 1.35 mol/L, and [H_2SO_4] 1 mol/L. The adsorption capacity of As(V) in AC is 9.1 mg As(V) /g AC; therefore, it can be seen that the presence of OMD greatly improves the absorption of As(V).

The mechanism of removing the As(V) in anionic form from water by the OMD/AC is complicated. The first stage is probably the formation of complexes on the surface of the AC, which is followed by ion exchange. The adsorption of anions has been related to reactions of complex formations on protonated sites or the presence of electrophilic sites. The As(V) is quite basic, suggesting that its adsorption in AC has a close relationship with the concentration of functional strong acid groups.

3. 5. Comparison of the Adsorption Data for Pb(II) and As(V)

One published review focused on adsorbents for the removal of arsenic, cadmium, and lead from contaminated waters.[50] Table 5 shows a comparison of the present work's data and some data from the literature for the same kind of adsorbent material. The adsorption capacity of OMD/CA is similar to that of Al_2O_3-pillared layered MnO_2 and Al-pillared montmorillonite (A, B) and better than that of other materials. Regarding the adsorption capacity of OMD/CA for As(V), the result obtained is not too low; though there are other materials with higher values of *q*.

4. Conclusions

The conditions for the synthesis of a material with MnO_2 (OMD) on activated carbon (AC) were studied. It can be deduced that mass-transfer phenomena in the range of the stirring speed (200–800 rpm) are not important. The oxidation rate increases according to the concentration of ozone in solution and the best conditions for attaining the lowest concentration of Mn(II) in solution which results in more deposits of manganese dioxide are 1.35 mol/L and 120 min of reaction. The rate of reaction of Mn(II) oxidation decreases with increased in sulfuric-acid concentration. Neither the concentration nor the particle size of AC influences the process of oxidation of Mn(II). Increasing temperature to 70 °C and a reaction time to greater than 60 min favors oxidation; for lower temperatures, oxidation is not significantly different.

For all experimental conditions agglomerates on AC were observed by means of SEM and EDS and the presence of manganese dioxide deposited on the surface of the AC was identified. The activation energy and the factor of frequency for the reaction were determined as E_a= 1.2 kcal/mol and A = 2.2, respectively. The value of E_a indicates that the precipitation of manganese dioxide in the AC is controlled by mass transfer in aqueous solution. The order of this reaction is zero.

The best conditions for the synthesis of OMD/AC to ensure maximum adsorption capacity for Pb(II) and

Table 5. Comparison of the adsorption capacities (*q*) of the materials in the present work and those of previously studied materials.

Material	*q* (mg Pb(II)/g)	Ref.	Material	*q* (mg As(V) /g)	Ref.
CA	14	This	CA	9.1	This
OMD/AC	90.5	work	OMD/AC	25.4	work
δ-MnO_2	27.81	51	Calcite/α-MnO_2	10.36	47
Al_2O_3-pillared layered MnO_2	80.22		Calcite/goethite/α-MnO_2	41.94	
Montmorillonite-K10	95–97	52	MnO_2 nanowires/diatomite	108.2	48
Al-pillared clay					
α-MnO_2	99.8%	53	Functionalized-nanoporous C/MnO_2	9.43	49
MnO_2/carbon nanotubes	6.7	54			
Silica/4-amino-2-mercaptopyridine	2.45 *μmol/g*	55			

As(V) were established. These values are 90.5 mg Pb(II)/g OMD/AC and 25.4 mg As(V)/g OMD/AC. When only AC is used, these values are: 14 mg Pb(II)/g AC and 9.1 mg As(V)/g AC. Therefore, the fixing of MnO_2 on the surface of the AC greatly improves the removal of Pb(II) and As(V) from aqueous solutions.

5. Acknowledgement

The authors would like to recognize the financing provided by CONACYT-Mexico in the form of Project No. 59989 and the scholarship awarded to E. Manríquez-Reza.

6. References

1. M. Fuentes, Arsénico en las Incrustaciones en las Redes de Distribución de Agua Potable en el Norte de México y su Desprendimiento, Agua Latinoamérica, Marzo/abril, 15, **2005**. http://www.bvsde.paho.org/bvsAIDIS/PuertoRico29/fuentes.pdf (assessed: January 27, 2017)
2. WHO, Air Quality Guidelines - Second Edition. Chapter 6.7 Lead, World Health Organization, Regional Office for Europe, Copenhagen, Denmark, **2001**. http://www.euro.who.int/__data/assets/pdf_file/ 0020/ 123077/ AQG2ndEd_6_7Lead.pdf (assessed: January 27, 2017)
3. F. N. Kemmer and J. McCallion, Manual del agua. Su naturaleza, tratamiento y aplicaciones. Tomo I, II. 1ra. ed. McGraw - Hill. México, **1989**. ISBN 9684225156
4. WHO. Guidelines for drinking-water quality [electronic resource]: incorporating first addendum. Vol. 1, Recommendations. – 3rd ed., World Health Organization, ISBN 92 4 154696 4, NML classification: WA 675, **2006**. http://www.who.int/water_sanitation_health/dwq/ gdwq 0506.pdf (assessed: January 27, 2017).
5. US-EPA, National Primary Drinking Water Regulations EPA 816-F-03-016 U.S. Environmental Protection Agency, **2003**. https://www.epa.gov/ground-water-and-drinking-water/table-regulated-drinking-water-contaminants (assessed: January 27, 2017)
6. Secretaria de Salud, Norma Oficial Mexicana NOM-127-SSA1-1994, Salud ambiental. Agua para uso y consumo humano. Límites permisibles de calidad y tratamientos a que debe someterse el agua para su potabilización, **2000**. http://www.gob.mx/cms/uploads/attachment/file/110534/NOM_127_SSA1_1994.pdf (assessed: January 27, 2017)
7. J. R. Conner, Chemical fixation and solidification of hazardous wastes, Springer Netherlands, **1990**. ISBN 978-0-442-20511-9
8. P. C. Hayes, Process Selection in extractive metallurgy, Hayes Publishing Co. **1985**. ISBN 0958919712
9. V. Lenoble, C. Laclautre, B. Serpaud, V. Deluchat and J. C. Bollinger, *Sci. Total Environ.*, **2004** *326(1-3)*, 197–207. http://dx.doi.org/10.1016/j.scitotenv.2003.12.012
10. V. Petkova, M. de L. Rivera, M. Piña, M. Avilés, and S. Pérez, Evaluación de diversos minerales para la remoción de arsénico de agua para consumo humano, Memorias técnicas. XI Congreso Nacional de Ingeniería Sanitaria y Ambiental. Zacatecas, 1 **1997**. http://www.zeocat.es/docs/aguaarsenico.pdf (assessed: January 31 2017)
11. M. L. Rivera and M. Piña, Tratamiento de agua para remoción de arsénico mediante adsorción sobre zeolita natural acondicionada, **2005**. http://www.zeocat.es/docs/aguaarsenico2.pdf (assessed: January 27, 2017)
12. US EPA, Technologies and Costs for Removal of Arsenic from Drinking Water, EPA 815R00028, Prepared by Malcolm Pirnie, Inc. under contract 68C60039 for EPA ORD, December **2000**. https://nepis.epa.gov/Exe/ZyPDF.cgi/P1004WDI.PDF?Dockey=P1004WDI.PDF (assessed: January 27, 2017)
13. US-EPA, Arsenic Treatment Technologies for soil, waste and water, U.S. Environmental Protection Agency, EPA-542-R-02-004, **2002**. https://www.epa.gov/sites/production/files/2015-04/documents/arsenic_report.pdf (assessed: January 31, 2017)
14. J. G. Parsons, M. L. Lopez, J. R. Peralta-Videa and J. L. Gardea-Torresdey, *Microchem. J.* **2009**, *91*, 100–106. http://dx.doi.org/10.1016/j.microc.2008.08.012
15. R. Contreras-Bustos, F. Espejel-Ayala, B. Cercado-Quezada, J. Jiménez-Becerril and M. Jiménez-Reyes, *Pol. J. Chem. Technol.* **2016,** *18*, 46–50. https://doi.org/10.1515/pjct-2016-0008
16. V. López-Ramón, C. Moreno-Castilla, J. Rivera-Utrilla and L.R. Radovic,*Carbon* **2002**, *41*, 2020–2022. http://dx.doi.org/10.1016/S0008-6223(03)00184-2
17. M. M. Rao, A. Ramesh, G. P. C. Rao and K. Seshaiah, *J. Hazard. Mater*. **2006**, *129*, 123–129. http://dx.doi.org/10.1016/j.jhazmat.2005.08.018
18. L. Beesley and M. Marmiroli, *Environ. Pollut*. **2011**, *159*, 474–480. http://dx.doi.org/10.1016/j.envpol.2010.10.016
19. A. Bogusz, P. Oleszczuk and R. Dobrowolski, *Bioresource Technol*. **2015**, *196*, 540–549. http://dx.doi.org/10.1016/j.biortech.2015.08.006
20. D. Dong, L. Liu, X. Hua and Y. Lu, *Microchem. J.* **2007**, *85*, 270–275. http://dx.doi.org/10.1016/j.microc.2006.06.015
21. L. Dong, Z. Zhu, H. Ma, Y. Qiu and J. Zhao, *J., Environ. Sci.* **2010**, *22*, 225–229. http://dx.doi.org/10.1016/S1001-0742(09)60097-8
22. A. Günay, E. Arslankaya and I. Tosun, *J. Hazard. Mater.* **2007**, *146*, 362–371. http://dx.doi.org/10.1016/j.jhazmat.2006.12.034
23. Z. Song, F. Lian, Z. Yu, L. Zhu, B. Xing and W. Qiu, *Chem. Eng. J.* **2014**, *242*, 36–42. http://dx.doi.org/10.1016/j.cej.2013.12.061
24. Y. Ren, N. Yan, J. Feng, J. Ma, Q. Wen, N. Li and Q. Dong, *Mater. Chem. Phys.* **2012**, *136*, 538–544. http://dx.doi.org/10.1016/j.matchemphys.2012.07.023
25. S. Wang, B. Gao, Y. Li, A. Meuse, A. R. Zimmerman, L. Q.

Ma, W. G. Harris and K. W. Migliaccio, *Bioresour. Technol.* **2015**, *181*, 13–17. http://dx.doi.org/10.1016/j.biortech.2015.01.044

26. L. M. Camacho, R. R. Parra and S. Deng, *J. Hazard. Mater.* **2011**, *189*, 286–293. http://dx.doi.org/10.1016/j.jhazmat.2011.02.035
27. R. Han, W. Zou, Z. Zhang, J. Shi and J. Yang, *J. Hazard. Mater.* **2006**, *137*, 384–395. http://dx.doi.org/10.1016/j.jhazmat.2006.02.021
28. S. Wang, W. Gong, X. Liu, Y. Yao, B. Gao and Q. Yue, *Sep. Purif. Technol.* **2017**, *58*, 17–23. http://dx.doi.org/10.1016/j.seppur.2007.07.006
29. Y. Wu, S. Yang, M. Zhang, A. Aierken and Y. Wu, *Korean J. Chem. Eng.* **2015**, *32*, 1667–1677. http://dx.doi.org/10.1007/s11814-014-0352-4
30. T. M. Albayati, G. M. Alwan and O. S. Mahdy, *Korean J. Chem. Eng.* **2017**, *34*, 259–265. http://dx.doi.org/10.1007/s11814-016-0231-2
31. N. Kijima, H. Yasuda, T. Sato and Y. Yoshimura, *J. Solid State Chem.* **2001**, *159*, 94–102. http://dx.doi.org/10.1006/jssc.2001.9136
32. R. Contreras and G. T. Lapidus, *J. Colloid Interf. Sci.* **1999**, *213*, 251–257. http://dx.doi.org/10.1006/jcis.1999.6114
33. C. Bigliocca, F. Girardi, J. Pauly,E. Sabbioni, S. Meloni and A. Provasoli, *Anal. Chem.* **1967**, *39*, 1634–1639. http://dx.doi.org/10.1021/ac50156a040
34. D. Glover, B. Schumm and A. Kozawa, Handbook of Manganese Dioxides Battery grade, International Battery Material Association (IBA Inc.), USA, **1989**.
35. R. Contreras, Producción de dióxido de manganeso por ozonización y estudio de sus propiedades de intercambio iónico, Doctoral dissertation, Universidad Autónoma Metropolitana, campus Iztapalapa, Mexico, **1999**. http://tesiuami.izt.uam.mx/uam/aspuam/presentatesis.php?recno=468&docs=UAM0468.PDF
36. K. Schaeffer, *Agua Latinoam.* **2003**, *3*, 1–5. http://www.agualatinoamerica.com/docs/pdf/Intermedio.pdf (assessed: January 31, 2017)
37. R. Leyva, L. G. Velázquez, J. Mendoza and R. M. Guerrero, *J. Mex. Chem. Soc.* **2002**, *46*, 159–166. http://www.redalyc.org/pdf/475/47546214.pdf
38. A. J. Rubin and D. L. Mercer, In: Adsorption of Inorganics at Solid-Liquid Interfaces; Anderson, M. A.; Rubin, A. J. Ed.; Ann Arbor Science Publishers Inc.: **1981**; p. 300.
39. H. Pérez, Modificación termoquímica y caracterización de un carbón activado lignítico, Barchelor dissertation, Universidad Veracruzana, **2006**.
40. I. Puigdomenech, **2010**. Program MEDUSA (Make Equilibrium Diagrams Using Sophisticated Algorithms). Royal Institute of Technology, Inorganic Chemistry, Stockholm, swedenignasi@inorg.kth.se.
41. M. Al-Anber and Z. A. Al-Anber, *Desalination* **2008**, *225*, 70–81. http://dx.doi.org/10.1016/j.desal.2007.07.006
42. M. Pourbaix, Atlas d'équilibres électrochimiques, Gauthier-Villars, Paris, **1963**.
43. C. Gottschalk, J. A. Libra and A. Saupe, Ozonation of water and waste water: A practical guide to understanding ozone and its applications, 2nd Ed., Wiley-VCH, Germany, **2010**. ISBN: 978-3-527-31962-6
44. J. L. Rodríguez-Santillán, T. Poznyak and J. L. Mayorga, Efecto del pH y Carbón Activado Sobre la Descomposición de Ozono en Solución Acuosa, In: XXVII Encuentro Nacional de la AMIDIQ, 2006. https://www.dropbox.com/s/57sdrecsy8amha3/2006.rar (assesed: January 31, 2017)
45. E. Peters and G. Bolton, *Hydrometallurgy: Theory and Practice*, Center for metallurgical and Process Engineering Department and Metallurgical Engineering, Chapter I, UBC. Vancouver, B. C. **1999**. ISBN-13: 978-0444896568
46. T. Nishimura and Y. Umetsu, *Shigen-to-Sozai* **1992**, *108*, 373–377. https://doi.org/10.2473/shigentosozai.108.373
47. Y. Umetsu, T. Nishimura and R. C. Bustos, M. Tokuda, *Shigen-to-Sozai* **2000**, *116,* 999–1004. https://doi.org/10.2473/shigentosozai.116.999
48. J. S. Markovski, V. Dokić, M. Milosavljević, M. Mitrić, A. A. Perić-Grujić, A. A., A. E. Onjia, A. D. Marinković, *Ultrason. Sonochem.* **2014**, *21*, 790–801. https://doi.org/10.1016/j.ultsonch.2013.10.006
49. Y. Du, G. Zheng, J. Wang, L. Wang, J. Wu, H. Dai, *Micropor. Mesopor. Mat.* **2014**, *200*, 27–34. https://doi.org/10.1016/j.micromeso.2014.07.043
50. S. Pathan, N. Pandita, N. Kishore, *Arabian J. Chem.* **2016** Available online 31 December 2016. http://doi.org/10.1016/j.arabjc.2016.12.011.
51. S. K. R. Yadanaparthi, D. Graybill, R. von Wandruszka, *J. Hazard. Mater.* **2009**, *171*, 1–15. https://doi.org/10.1016/j.jhazmat.2009.05.103
52. H. Zhang, L. Gu, L. Zhang, S. Zheng, H. Wan, J. Sun, D. Zhu, Z. Xu, *Appl. Surf. Sci.* **2017**, *406*, 330–338.
53. D. Humelnicu, M. Ignat, M. Suchea, *Acta Chim. Slov.* **2015,** *62*, 947–957. https://doi.org/10.17344/acsi.2014.1825
54. S. T. El-Wakeel, R. S. El-Tawil, H. A. M. Abuzeid, A. E. Abdel-Ghany, A. M. Hashem, *J. Taiwan Inst. Chem. Eng.* **2017**, *72*, 95–103.
55. B. Yang, Q. Gong, L. Zhao, H. Sun, N. Ren, J. Qin, J. Xu, H. Yang, *Desalination* **2011**, *278*, 65–69. https://doi.org/10.1016/j.desal.2011.05.010

Povzetek

Proučili smo pogoje za pripravo materialov z MnO_2 (OMD) na aktivnem oglju (AC) in sicer reakcijski čas, temperaturo, hitrost mešanja, koncentracije AC, H_2SO_4 in O_3 v raztopinah ter velikost delcev. Aglomerate na AC smo spremljali zvrstičnim elektronskim mikroskopom (SEM) in z mikroanalizo z energijsko disperzijsko spektroskopijo (EDS) potrdili prisotnost OMD depozitov na površini. Izračunali smo aktivacijsko energijo in frekvenčni faktor reakcije $E_a = 1.2$ kcal/mol in $A = 2.2$. Vrednost E_a kaže, da je nalaganje OMD na AC kontroliran z masnim prenosom v vodnih raztopinah, reakcija je ničtega reda.

Adsorpcijska kapaciteta AC je $q = 14$ mg Pb(II)/g AC in $q = 9.1$ mg As(V)/g AC. Adsorpcijska kapaciteta na sistemu OMD/AC pri sledečih pogojih: [AC] 1 ali 2 g/L, velikost delcev AC +0.59 mm, [H_2SO_4] 1 ali 2 mol/L, 25 °C, hitrost mešanja 600 rpm, in [O_3] 1.35 mol/L je $q = 90.5$ mg Pb(II)/g OMD/AC in 25.4 mg As(V)/g OMD/AC. Vezava OMD na površino AC torej izredno izboljša odstranjevanje Pb(II) in As(V) iz vodnih raztopin.